has been found to scale with crystal size, L, approximately as $1/L^{\gamma}$, with γ in the range 1.2–1.8. These calculations are consistent with our quantum-confinement interpretation.

The room-temperature photoluminscence (PL) properties of these superlattices was measured by using an 80-mW 457.9-nm argon laser beam as the excitation source, and by using a Photometrics CCD 9000 Si array detector to detect the luminescence which was dispersed by a Spex 1877C triple spectrometer. A PL peak at wavelengths across the visible range was observed from superlattices with Si film thicknesses $\leqslant 3$ nm. A typical PL spectrum is shown in Fig. 4 inset. We could not detect any PL signal from superlattices with Si film thickness >3 nm. This may be explained as due to a dramatic reduction in the quantum confinement effects, as shown in Fig. 3. The PL peak energy as a function of the Si thickness is plotted in Fig. 4. The peak energy position, E_{PL}, was found to be best-fitted by E_{PL} (eV) = $1.6 + 0.7/d_{Si}^2$. According to effective mass quantum-confinement theory, 1.6 eV corresponds to the band gap of bulk material. This fitted value is certainly larger than that of crystalline silicon, but is in good agreement with that of bulk non-crystalline silicon (1.5–1.6 eV at 295 K)[18]. Thus the PL data further confirm that quantum confinement governs the Si energy band structure and is the fundamental source of the bright Si luminescence. It should be possible to tune the wavelength of the emitted light by varying the Si film thickness, which can be fabricated with atomic-layer precision by modern molecular-beam epitaxy technology. □

Received 30 August; accepted 6 October 1995.

1. Iyer, S. S. & Xie, Y.-H. *Science* **260,** 40–46 (1993).
2. Abeles, B. & Tiedje, T. *Phys. Rev. Lett.* **51,** 2003–2006 (1983).
3. Wilson, W. L., Szajowski, P. F. & Brus, L. E. *Science* **262,** 1242–1244 (1993).
4. Canham, L. T. *Appl. Phys. Lett.* **57,** 1046–1048 (1990).
5. Cullis, A. G. & Canham, L. T. *Nature* **353,** 335–338 (1991).
6. Lehmann, V. & Gösele, U. *Appl. Phys. Lett.* **58,** 856–858 (1991).
7. Halimaoui, A. *et al. Appl. Phys. Lett.* **59,** 304–306 (1991).
8. Petrova-Koch, V. *et al. Appl. Phys. Lett.* **61,** 943–945 (1992).
9. Proot, J. P., Delerue, C. & Allan, G. *Appl. Phys. Lett.* **61,** 1948–1950 (1992).
10. Van de Walle, C. G. & Northrup, J. E. *Phys. Rev. Lett.* **70,** 1116–1119 (1993).
11. Van Buuren, T. *et al. Appl. Phys. Lett.* **63,** 2911–2914 (1993).
12. Hybertsen, M. S. *Phys. Rev. Lett.* **72,** 1514–1517 (1994).
13. Baribeau, J.-M., Lockwood, D. J. & Lu, Z. H. *Mater. Res. Soc. Symp. Proc.* Vol. 382 (Materials Research Society, Pittsburg, in the press).
14. Lu, Z. H. & Yelon, A. *Phys. Rev.* B41, 3284–3286 (1990).
15. Lu, Z. H., Baribeau, J.-M. & Jackman, T. E. *Can. J. Phys.* **70,** 799–802 (1992).
16. Lockwood, D. J. *et al. Can. J. Phys.* **70,** 1184–1193 (1992).
17. Tsu, R. *Nature* **364,** 19 (1993).
18. Street, R. A. & Biegelsen, D. K. in *The Physics of Hydrogenated Amorphous Silicon* (eds Joannopoulos, J. D. & Lucovsky, G.) 195–259 (Springer, Berlin, 1984).

ACKNOWLEDGEMENTS. We thank J. P. McCaffrey for TEM measurements, H. J. Labbé for PL measurements, and K. H. Tan for assisting with synchrotron measurements at the US NSF funded Synchrotron Radiation Center. Z.H.L. thanks T. Tiedje for sending his relevant works, and A. Yelon, M. S. Hybertsen and Y. H. Xie for many useful discussions.

Femtosecond molecular dynamics of tautomerization in model base pairs

A. Douhal, S. K. Kim & A. H. Zewail

Arthur Amos Noyes Laboratory of Chemical Physics, California Institute of Technology, Pasadena, California 91125, USA

HYDROGEN bonds commonly lend robustness and directionality to molecular recognition processes and supramolecular structures[1,2]. In particular, the two or three hydrogen bonds in Watson–Crick base pairs bind the double-stranded DNA helix and determine the complementarity of the pairing. Watson and Crick pointed out[3], however, that the possible tautomers of base pairs, in which hydrogen atoms become attached to the donor atom of the hydrogen bond, might disturb the genetic code, as the tautomer is capable of pairing with different partners. But the dynamics of hydrogen bonds in general, and of this tautomerization process in particular, are not well understood. Here we report observations of the femtosecond dynamics of tautomerization in model base pairs (7-azaindole dimers) containing two hydrogen bonds. Because of the femtosecond resolution of proton motions, we are able to examine the cooperativity of formation of the tautomer (in which the protons on each base are shifted sequentially to the other base), and to determine the characteristic timescales of the motions in a solvent-free environment. We find that the first step occurs on a timescale of a few hundred femtoseconds, whereas the second step, to form the full tautomer, is much slower, taking place within several picoseconds; the timescales are changed significantly by replacing hydrogen with deuterium. These results establish the molecular basis of the dynamics and the role of quantum tunnelling.

There are two possible mechanisms of double proton transfer in these model base pairs: a stepwise transfer from the base-pair structure (B-PS) to the tautomer structure (TS) through an intermediate (zwitterionic) structure (IS), or a direct cooperative transfer of B-PS to TS (Fig. 1*a*). Since the seminal work by Taylor, El Bayoumi and Kasha[4], experimental evidence of a photoinduced proton-transfer reaction in solution and matrices at 4.2 K (refs 4, 5) as well as in a supersonic-jet expansions[6], has been reported. In solution, the first picosecond study[7] showed that the transfer occurs in less than 5 ps. Subpicosecond[8] studies have recently been reported and showed an excited-state lifetime of 1.4 ps in hexadecane at room temperature. The issue of cooperativity or concertedness of the motion must take into account the role of the solvent and the intramolecular dynamics.

Our experimental system is shown in Fig. 1*b*. An initial ultraviolet femtosecond (fs) pulse (305–310 nm) excites the base pair (formed in a molecular beam to avoid collisional deactivation and other intermolecular perturbations) to the first electronically excited state, defining a zero of time. A second fs pulse (~620 nm), delayed in time, probes the dynamics of the pair by exciting the bases above their ionization threshold, so that they can then be monitored by time-of-flight (TOF) mass spectrometry. As with other fs studies[9], the zero of time can be established *in situ* by identifying the ion signal that results when the two pulses coincide. We have also studied the effect of deuterium substitution to examine possible quantum tunnelling effects of the motion.

Figure 2 shows the TOF mass spectra obtained when exciting and probing pulses at no delay ($t = 0$); the ionization potential of the monomer is 8.11 eV (ref. 6). The mass peaks at 118 and 236 correspond to the monomer and to the dimer of 7-azaindole, respectively. Figure 2 also gives the corresponding spectra of the deuterated species of NH and CH bonds, assigned on the basis of the stronger acidity of NH relative to CH (ref. 10).

Figure 3 shows the fs transients for the fully undeuterated (NH,NH,CH) pair at two different vibrational energies, E, above the zero-point energy[6]. For the dimer, the decay was fitted to a bi-exponential function, giving decay times of $\tau_1 = 650$ fs and $\tau_2 = 3.3$ ps when $E = 0$. For $E \approx 1.5$ kcal mol^{-1}, these rates changed significantly giving $\tau_1 = 200$ fs and $\tau_2 = 1.6$ ps, indicating the presence of a reaction barrier. (We could not obtain an accurate fit of the full decay when a single exponential behaviour was assumed; Fig. 3.)

For a cooperative, single-step change of the base-pair structure to the tautomer structure, only a single exponential decay is expected, even with a reversible process. In contrast, a two-step process,

$$\text{B-PS} \overset{k_1}{\rightarrow} \text{IS} \overset{k_2}{\rightarrow} \text{TS} \qquad (1)$$

will give rise to bi-exponential transients, reflecting the decay (with k_1) of B-PS and the build-up (k_1) and decay (k_2) of IS (note that TS has a nanosecond lifetime, so its decay is not

© 1995 Nature Publishing Group

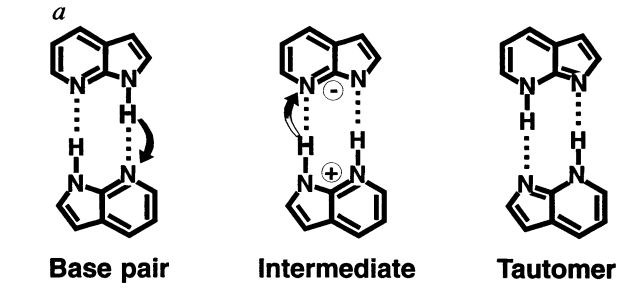

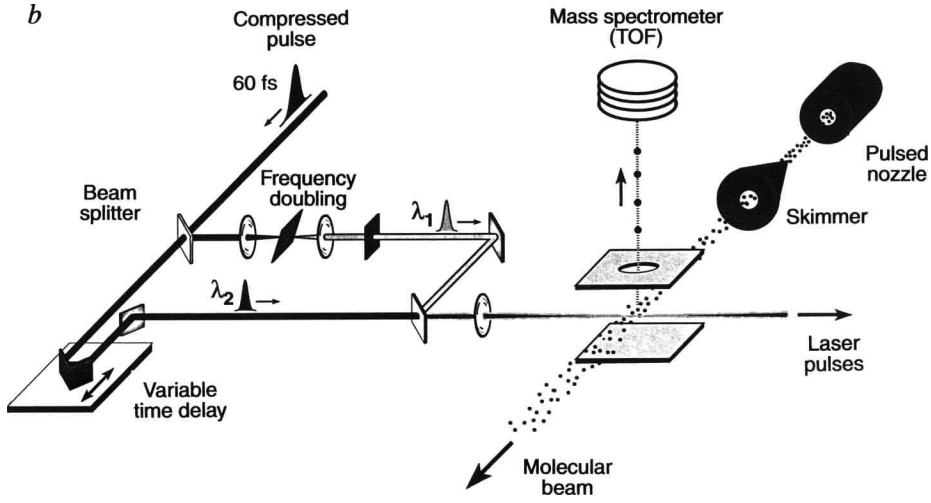

FIG. 1 *a*, The molecular structures involved in the two-step, or one-step, cooperative double proton transfer dynamics of the base pair (7-azaindole dimer); *b*, schematic diagram of part of the experimental apparatus showing the generation of the femtosecond (λ_1, pump; λ_2, probe) pulses (ref. 9, pages 120–134) and the skimmed molecular beam (ref. 9, pages 319–327), together with the detection compartment which uses time-of-flight mass spectrometry. The compressed, amplified pulses were 60 fs in duration and had an energy of ~0.5 mJ. The cross-correlation of the pump and probe pulses was measured *in situ* to be ~150 fs. The power of the pulses were controlled to study their effect on the transients.

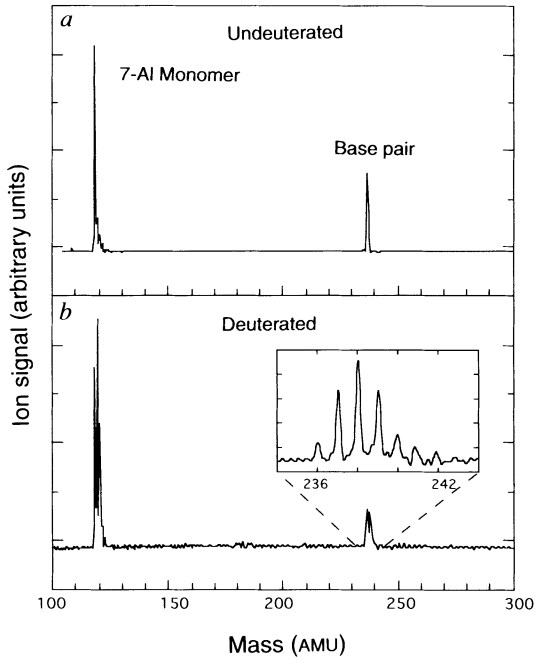

FIG. 2 Time-of-flight mass spectra of the (upper panel) undeuterated and (lower panel) deuterated pair at zero-time delay. The masses at 118 and 236 AMU are due to ions of monomer and base pair, respectively. Mass 236 corresponds to the undeuterated pair, labelled (NH,NH,CH); mass 237 to a mono-deuterated pair, most probably predominantly of type (ND,NH,CH); mass 238, which is the most intense one, is due to the di-deuterated pair, assigned to the (ND,ND,CH) species. The other observed peaks at higher masses (239, 240, 241 and 242) show the existence of 3, 4, 5 and 6 deuterium atoms in the pair indicating the deuteration of both the NH and CH bonds. To form the molecular beam, 7-azaindole (98%, Aldrich) was heated to 373 K with a backing pressure of helium (~300 torr). Special care in optimizing the conditions of the beam was made to form the pair; details will be published elsewhere. The skimmer aperture was 2 mm and the nozzle diameter was 0.3 mm. Deuteration was carried out by dissolving the parent compound in a mixture of acetone–D_2O which was later evaporated at 333 K under vacuum.

© 1995 Nature Publishing Group

evident on these timescales). As all of these structures have the same mass, they all contribute to the dimer mass peak, but with different cross-sections for ionization (as in other mass-detection experiments[9]). The fact that the initial tautomerization is on the fs timescale, when the total vibrational energy is zero, indicates that the proton transfer motion is direct and does not involve the entire vibrational phase space of the pair. The implication is that the motion can be described as being 'localized' in the coordinate of N–H $\cdots$ N.

The rate of tautomerization can be modelled by considering the tunnelling motion (rate constant k) of the proton in a double-well potential, with the system either in the N–H or the NH^+ configuration of the two moieties:

$$k = \nu \exp\left[-\pi a\sqrt{2mU_0}\right] \qquad (2)$$

where ν is reaction-coordinate frequency (N–H), $a_0 = \hbar a$ is the half-width of the energy barrier and U_0 is its height, and m is the effective mass of the particle. Using the measured k and taking ν for the N–H vibration of 2,800 cm^{-1} and $a_0 = 0.27$ Å (ref. 5), we obtained $U_0 = 1.2$ kcal mol^{-1}. This model assumes that the distance between the two nitrogens is fixed. When relaxing this condition and averaging over the stretch motion of the N $\cdots$ N centres (two-dimensional model) at $E = 0$ we again obtained $U_0 \approx 1.3$ kcal mol^{-1}. For self-consistency, we have repeated these two types of calculations[11] and obtained satisfactory agreement for the effect of isotope substitution and also for the excess vibrational energy, as discussed below.

Löwdin[12] has discussed the theoretical description of the double-well process and its relevance to genetics. One consequence of this process of barrier tunnelling[13] is the effect on the rates by changing m by deuteration. As shown in Fig. 4, the 360-fs component changes to 3 ps on deuteration. This change is totally consistent with the above calculation when changing $m = 1$ (H) to $m = 2$ (D). In the two-dimensional model, for example for E corresponding to two quanta of the N $\cdots$ N stretch (0.7 kcal mol^{-1}), we obtained a k^{-1} value of 300 fs for the proton transfer and 5.5 ps for the deuteron transfer, consistent with the experimental trends.

The ps component characterizes the decay of the IS to the final tautomer. From the energy dependence and isotope effect (Figs 3 and 4) we obtain a barrier height using the above procedure; from the rates, a lower limit of 2.6 kcal mol^{-1} is obtained for this second step. This barrier height is larger than that of the first step, which is reflected in the fact that the characteristic timescale is of the order of picoseconds rather than femtoseconds.

With the equivalence of the two hydrogen bonds in the static structure of the pair it is interesting to consider the nature of the process that leads to the dynamical structures. We propose the following model. Because the timescale of the proton motion is observed to be relatively short, compared to the energy redistribution[14], the 'reaction centre' involves primarily the N–H and N $\cdots$ N intermolecular motions. The timescale of the proton motions, however, is longer than (or comparable to) the changes in the electronic distribution on excitation and the nuclear vibrational motions of the N–H and N $\cdots$ N stretches. This last inequality allows for the asymmetric motion of one of the protons, and, because one moiety is excited, the proton ultimately

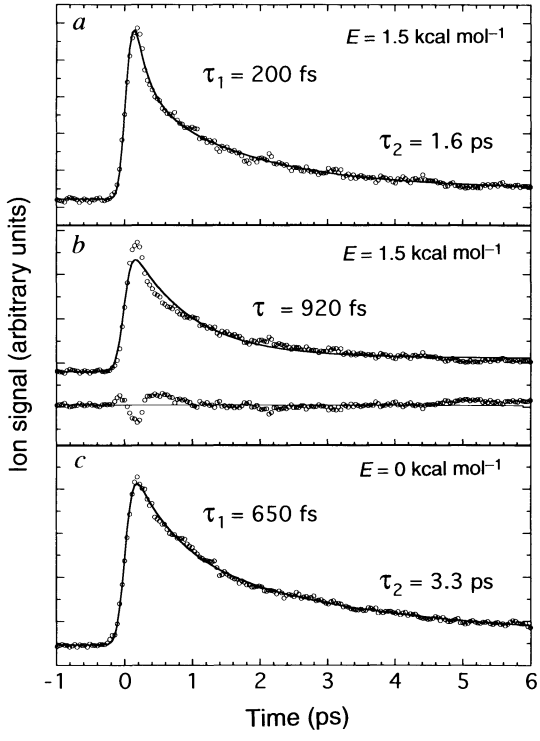

FIG. 3 Femtosecond transients of the base pair (236 AMU) as a function of the time delay. *a*, Excitation with an excess vibrational energy $E \approx 1.5$ kcal mol^{-1}; *b*, a single exponential fit of the same data; and *c*, excitation with $E \approx 0$. A bi-exponential function (and a small constant background) is used to fit both decays in *a* and *c*. The constant takes into account the nanosecond decay, a contribution of ~10%, of the total signal. Note the distribution of residuals (lower trace) in *b* when a single exponential decay is assumed. The observed transient is not power-dependent, and only one ultraviolet photon excitation is responsible for the observed dynamics.

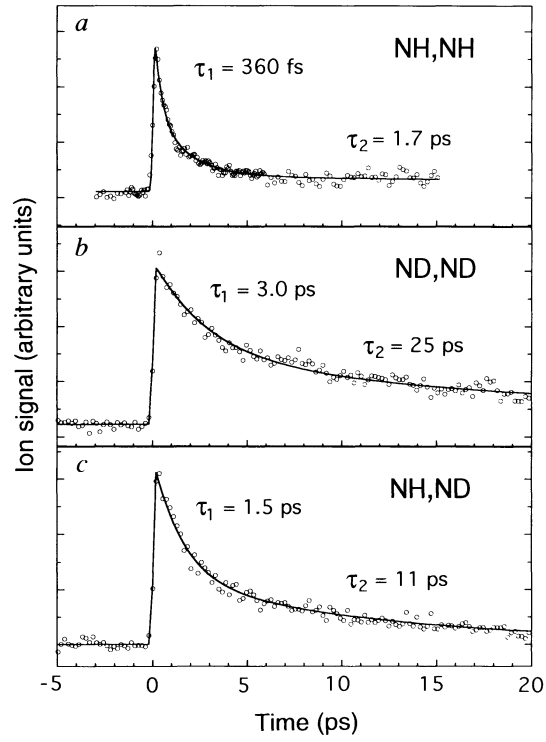

FIG. 4 Femtosecond transients of the ion signal of the base pair (NH,NH,CH) (*a*), (ND,ND,CH) (*b*) and (ND,NH,CH) (*c*) as a function of the time delay with $E \approx 1$ kcal mol^{-1}. To obtain accurate values of the slow component, τ_2, data from scans with longer time delays (60 ps) were taken and analysed.

© 1995 Nature Publishing Group

transfers, leading to the IS. A consequence of this transfer is stability for the second N–H motion and a higher barrier toward TS formation. The N···N stretch has been assigned[6] the value 120 cm^{-1} and the N–H stretch is about 2,800 cm^{-1}, giving 280 and 12 fs, respectively. Therefore, on the timescale of 0.5–10 ps (typical reaction times) the 'asymmetric reaction coordinate' for the two particles is established.

To further probe this picture we have examined the transient behaviour of the pair with NH,ND composition. A comparison of the transient behaviour of three species is made in Fig. 4. It is remarkable that the (ND,NH,CH) species gives rates 'in between' the values of the (NH,NH,CH) and (ND,ND,CH) species. This behaviour can be understood by considering the breakage of the phase in the vibrational motion of the two N–H bonds. Considering 50% probability for exciting either part of the base pair, we deduce effective time constants of ~1 ps and ~20 ps which describe the experimental trend reasonably well. Interestingly, for the (ND,ND,CD) species, with presumably one deuterium on the carbon rings, the transient behaviour is very similar to that of the (ND,ND,CH) species, again consistent with the locality of the dynamics in the hydrogen-bond regions.

The process of mutation by tautomerization[3] is similar to the excited-state process described here. If a 'misprint' induced by a tautomer takes place during replication[15,16], then an error is recorded. Because reaction-path calculations of DNA base pairs[17] show similar potential energy characteristics to those discussed here, we anticipate being able to explore the relevance of tautomerization dynamics to mutagenesis. □

Received 7 September; accepted 25 October 1995.

1. Zewail, A. (ed.) *The Chemical Bond: Structure and Dynamics* (Academic, San Diego, 1992).
2. Ball, P. *Designing the Molecular World* (Princeton Univ. Press, 1994).
3. Watson, J. D. H. & Crick, F. H. C. *Nature* **171,** 737–738 (1953).
4. Taylor, C. A., El Bayoumi, M. A. & Kasha, M. *Proc. natn. Acad. Sci. U.S.A.* **63,** 253–260 (1969).
5. Ingham, K. C. & El-Bayoumi, M. A. *J. Am. chem. Soc.* **96,** 1674–1682 (1974).
6. Fuke, K. & Kaya, K. *J. phys. Chem.* **93,** 614–621 (1989).
7. Hetherington, W. M., Micheels, R. H. & Eisenthal, K. B. *Chem. Phys. Lett.* **66,** 230–233 (1979).
8. Share, P., Pereira, M., Sarisky, M., Repinec, S. & Hochstrasser, R. M. *J. Luminescence* **48/49,** 204–208 (1991).
9. Zewail, A. H. *Femtochemistry: Ultrafast Dynamics of the Chemical Bond* (World Scientific, Singapore, 1994).
10. Yu, H.-T., Colucci, W. J., Mclaughlin, M. L. & Barkley, M. D. *J. Am. chem. Soc.* **114,** 8449–8454 (1992).
11. Kim, S. K. *et al. J. phys. Chem.* **99,** 7421–7435 (1995).
12. Löwdin, P.-O. *Adv. Quantum Chem.* **2,** 213–361 (1965).
13. Benderskii, V. A. & Goldanskii, V. I. *Int. Rev. phys. Chem.* **11,** 1–70 (1992).
14. Herek, J. L., Pedersen, S., Bañares, L. & Zewail, A. H. *J. chem. Phys.* **97,** 9046–9061 (1992).
15. Cairns, J. *J. molec. Biol.* **6,** 208–213 (1963).
16. Stryer, L. *Biochemistry* 3rd edn (Freeman, New York, 1988).
17. Rein, R. & Harris, F. E. *J. chem. Phys.* **42,** 2177–2180 (1965).

ACKNOWLEDGEMENTS. A. Douhal is on leave from the Universidad de Castilla-La Mancha (Spain), and thanks that university and the California Institute of Technology (USA) for support and for making possible a fruitful stay at Caltech. We thank S. Pedersen for his help with Fig. 1. This work was supported by the US Air Force Office of Scientific Research and the US NSF.

Cell-free synthesis of polyketides by recombinant erythromycin polyketide synthases

Rembert Pieper*, Guanglin Luo†, David E. Cane† & C. Khosla*‡

*Department of Chemical Engineering, Stanford University, Stanford, California 94305-5025, USA
†Department of Chemistry, Brown University, Box H, Providence, Rhode Island 02912, USA

MODULAR polyketide synthases (PKSs) are complex multi-enzyme proteins that catalyse the bacterial biosynthesis of many pharmaceutically useful polyketides. The PKSs are organized into a series of modules, each containing the active catalytic sites required for one step in the synthesis process[1–4]. Here we report a method for cell-free enzymatic synthesis of 6-deoxyerythronolide B (6-dEB), the parent molecule of the antibiotic erythromycin A, using recombinant 6-deoxyerythronolide B synthase (DEBS), a modular PKS with at least 28 distinct active sites. We have also synthesized *in vitro* a triketide lactone by using a truncated mutant of DEBS. The availability of such cell-free synthetic routes will allow direct investigation of the structural and mechanistic basis for the unusual combination of high substrate specificity[5–10] and tolerance to genetic reprogramming[2,11–15] found in this enzyme family.

Polyketides are synthesized in a manner analogous to fatty-acid biosynthesis[16] in which carbon chains are built by successive condensations between monomers such as acetate, propionate and butyrate. After each condensation reaction, the resulting β-carbonyl undergoes all, part or none of a reductive cycle comprising β-ketoreduction, dehydration, and enoyl reduction[17,18]. Thus structural diversity in this family of natural products arises from variations in the choice of monomers, the extent of the β-ketoreduction that occurs during each condensation cycle, the stereochemistry of each chiral carbon centre, and the regiochemistry of cyclization reactions that occur after chain synthesis is completed.

The PKS 6-deoxyerythronolide B synthase (DEBS) consists of three multifunctional proteins, DEBS 1, DEBS 2 and DEBS 3, each of which possesses two modules (Fig. 1). The PKS-mediated process of complex polyketide biosynthesis has been explored by radioisotope and stable isotope labelling experiments[5–10] (see ref. 17 for review), heterologous expression[19], directed mutagenesis[2,11–15], and *in vitro* studies on partly active proteins (ref. 20 and references therein). But cell-free enzymatic synthesis of complex polyketides has proved unsuccessful despite more than 30 years of intense efforts[21–23] (the claim in ref. 24 to have observed cell-free synthesis of 6-dEB has not been followed by any supporting published data), presumably because of the difficulties in isolating fully active forms of these large, poorly expressed multifunctional proteins from naturally occurring producer organisms, and because of the relative lability of intermediates formed during the course of polyketide biosynthesis. The three DEBS proteins have been purified individually from the natural producer organism, *Saccharoployspora erythrea*[25], and studies of the purified enzymes facilitated clarification of their stereospecificity. However, the absence of chain-elongation activity in these preparations prevented detailed investigations of the mechanisms of this enzyme complex. In an attempt to overcome some of these limitations, modular PKS subunits have been expressed in heterologous hosts such as *Escherichia coli* (ref. 26 and references therein) and *Streptomyces coelicolor*[19]. Whereas the proteins expressed in *E. coli* are not fully active, heterologous expression of the DEBS PKS in *S. coelicolor* resulted in production of active protein, as demonstrated by the production of 6-dEB *in vivo*. Cell-free enzymatic synthesis of polyketides from PKSs with substantially fewer active sites, such as the 6-methylsalicylate synthase[27], chalcone synthase[28], tetracenomycin synthase[29], and the PKS responsible for the polyketide component of cyclosporin[30], have also been reported.

Here we have focused on polyketide synthesis by recombinant DEBS and by an active deletion mutant whose construction has previously been reported[13,15]. The deletion mutant, designated 'DEBS 1 + TE', contains the first two modules from DEBS 1 fused to the thioesterase domain normally found at the carboxy-terminal end of module 6 of DEBS (Fig. 1). Both the complete

‡To whom correspondence should be addressed.

© 1995 Nature Publishing Group